Magnetic-moment distribution and superlattice dislocations in the $L1_2$-type structure

Seiki Takahashi
Faculty of Engineering, Iwate University, Morioka, Iwate, Japan

Kôki Ikeda*
Laboratoire de Physique des Solides, Université de Paris—Sud, F-91405 Orsay, France
(Received 9 June 1983)

The transition of magnetic structure due to plastic deformation in the $L1_2$-type ordered alloys and compounds is explained in terms of the modified slip-induced directional-order model with consideration of magnetic interactions between the neighboring atoms. The environment of each atom after plastic deformation is elucidated. The change of the atomic environment on plastic deformation produces the magnetic transition from ferromagnetism to antiferromagnetism or vice versa. The magnetization of the plastically deformed alloys is formulated as the function of the dislocation density. Numerical estimates are given for the Pt_3Fe, Pt_3Co, Ni_3Fe, and Ni_3Mn alloys and for the Ni_3Al intermetallic compound.

I. INTRODUCTION

Local magnetic effects have been studied by many investigators experimentally and theoretically in the chemically ordered alloys. One of their interests is the magnetic behaviors of atoms due to their environment. To investigate the relationship between the magnetic properties of atoms and their environment experimentally, the magnetic properties have been compared in the chemically ordered and disordered states or the magnetic measurements have been carried out, adding the excess atoms to the stoichiometric ordered alloys. As one of the methods to make the chemically disordered state, we give an application of plastic deformation to the specimens, grinding or powdering by means of a file. However, this method has not been adopted in general because of the lack of the information about the atomic environment after plastic deformation. It is possible to get the accurate information. In this paper, the atomic environment after plastic deformation will be elucidated.

Several remarkable magnetic phenomena due to plastic deformation were discovered in the chemically ordered alloys. The Pt_3Fe alloy is antiferromagnetic when ordered and ferromagnetic when disordered in the superlattice region.[1,2] It was discovered that in the long-range-ordered Pt_3Fe alloy, which showed no ferromagnetism before plastic deformation, the application of plastic deformation caused it to become quite strongly ferromagnetic even at room temperature.[1] It was found that in the ordered Ni_3Mn alloy, the saturation magnetization decreases with the amount of elongation, while in the ordered Pt_3Co alloy, the intensity of magnetization increases with the amount of compression.[3] The Ni_3Al intermetallic compound shows very weak itinerant ferromagnetism as an example of the Stoner-Edwards-Wohlfarth model.[4] It was shown in this compound that the disordering due to plastic deformation causes the susceptibility as well as the magnetization to reduce considerably.[4]

Recently, a remarkable reduction of the magnetization has been also discovered in the plastically deformed Pd_2MnSn alloy. And the reduction in magnetization recovers by the 300 °C annealing and recovers completely by the 800 °C annealing.[5] The reduction of magnetization has been successfully explained by use of the modified slip-induced directional-order model,[6,7] with consideration of ferromagnetic and antiferromagnetic interactions between Mn atoms.[8]

In the present study, the method applied to the Pd_2MnSn Heusler alloy is extended to the magnetic behaviors of the $L1_2$-type alloys and compound on plastic deformation. The mechanism of the transition of magnetic structure on plastic deformation will be elucidated and

TABLE I. Number of neighboring atoms around the host atoms in the A_3B alloys and compounds with $L1_2$-type, before and after plastic deformation. There are two kinds of host A atoms with different number of the NN atoms near the APB.

Host atoms \ Neighboring atoms		At first NN		At second NN		At third NN		At fourth NN		At fifth NN		At sixth NN	
		A	*B*	*A*	*B*	*A*	*B*	*A*	*B*	*A*	*B*	*A*	*B*
Normal state	Around *A* atom	8	4	6	0	16	8	12	0	16	8	8	0
	Around *B* atom	12	0	0	6	24	0	0	12	24	0	0	8
APB	Around *A* atom												
	at *F* site	8	4	6	0	16	8	12	0	16	8	8	0
	at *C* site	9	3	3	3	19	5	9	3	20	4	3	5
	Around *B* atom	11	1	3	3	21	3	3	9	20	4	4	4

the net magnetization of the plastically deformed crystals with the $L1_2$ structure will be formulated as the function of the dislocation density. The numerical estimation in the magnetization will be given to four alloys and a compound with $L1_2$-type structure: Pt_3Fe, Pt_3Co, Ni_3Mn, Ni_3Fe, and Ni_3Al.

II. CRYSTAL STRUCTURE AND SUPERLATTICE DISLOCATION

The long-range-ordered A_3B alloy of the $L1_2$-type has such the structure that A and B atoms occupy the face-centered and corner sites, respectively, in fcc structure. Each B atom is surrounded by twelve A atoms at the first nearest neighbor (NN) (Table I). By plastic deformation, dislocations nucleate, slip over the glide plane, and make the configuration of these atoms change.

There is a repulsive force between two dislocations with the same Burgers vector, and the wider the distance between them, the more stable their interaction in usual crystals. The dislocation in long-range-ordered alloys, however, creates an antiphase boundary (APB) over the glide plane after it has slipped and it is stable to make a pair with another dislocation. Figure 1 shows the generation of an APB by the passage of a dislocation in an ordered alloy in a two-dimensional model. The spacing between paired dislocations is given by the APB energy and the elastic interaction energy between individual dislocations. Superlattice dislocations in the $L1_2$-type long-range-ordered alloys were studied in detail by Marcinkowski *et al.*[9] They are shown schematically in Fig. 2, where one perfect dislocation with $(a/2)[01\bar{1}]$ Burgers vector separates into two paired dislocations with $(a/6)\langle 211\rangle$ Burgers vectors, where a is the lattice constant. Between perfect dislocations there exists an APB over the (111) glide plane, while there exist APB's and a stacking fault between partial dislocations. The separation of partial dislocations r_1 is expected to be much smaller than that of perfect dislocations r. These separations will take the constant values. We will call these dislocations a-type superlattice dislocation. The a-type superlattice dislocations are expected to be observable in the initial stage of plastic deformation.

Another type of superlattice dislocation can be introduced, which does not have a constant value as the separation r, and does distribute independently free from the attractive force due to the APB energy. These superlattice dislocations are expected to be observable in the advanced stage of plastic deformation. They are called b-type superlattice dislocation in this paper.

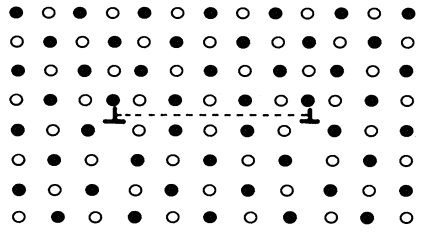

FIG. 1. Generation of an APB by the passage of a dislocation in an ordered state: two-dimensional model.

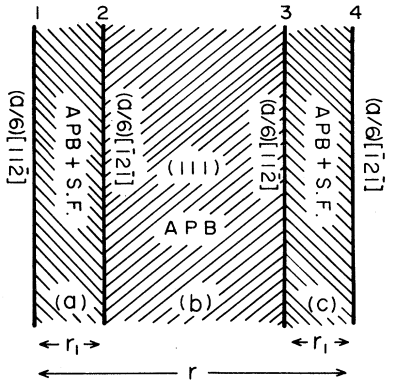

FIG. 2. Schematic structure of superlattice dislocations over the (111) glide plane in the $L1_2$-type structure. $(a/2)[01\bar{1}]$ perfect dislocation separates into two partial dislocations with $(a/6)\langle 211\rangle$ Burgers vector.

At first the effect of partial dislocations is neglected. The dislocations are created by plastic deformation; the first perfect dislocation makes an APB over the glide plane and the next dislocation makes the glide plane recover. The APB between these dislocations remains over the glide plane. Across the APB which is induced by plastic deformation, the first- and second-NN atoms are altered in such a manner that the B-B atom pairs appear in the first NN. The environment of each atom changes before and after plastic deformation and is shown in Table I.

The superlattice dislocations are accompanied by the APB over the $\{111\}$ glide plane. The APB and the initial state alternate over the glide plane after plastic deformation. The area of the APB, induced by plastic deformation, is given by

$$A = \int_v r\, ds \ , \tag{1}$$

where r is the separation between two dislocations composing the APB and ds is a segment of one of these dislo-

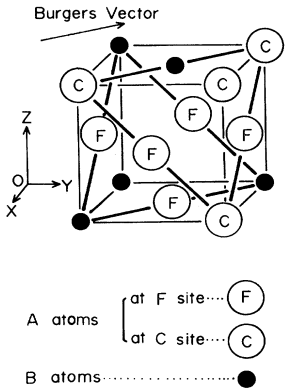

FIG. 3. Atomic arrangement of the $L1_2$-type structure after the $(a/2)[\bar{1}10]$ dislocation slips over the (111) glide plane. APB distributes over the (111) glide plane.

cations as shown in Fig. 3. The integral is performed over the entire specimen. The number of B-B atom pairs per unit area in the $\{111\}$ plane, which are located in the first NN is $1/\sqrt{3}a^2$, and the number of B atoms at the "irregular" site is given by

$$n=\frac{2S^2}{\sqrt{3}a^2}A \ , \tag{2}$$

where S is the long-range order parameter before the specimen is plastically deformed. The number of B atoms at the irregular site per unit volume is given by

$$n=\frac{S^2}{\sqrt{3}a^2}\bar{r}\rho \ . \tag{3}$$

Here ρ is the dislocation density, which is defined as the whole dislocation length per unit volume and $\bar{r}$ is the average of r. The separation $\bar{r}$ for a-type superlattice dislocations is given by

$$S^2\bar{r}=\frac{Gb^2}{2\pi E_{\rm APB}}\left[\frac{\cos^2\psi}{1-\nu}+\sin^2\psi\right] , \tag{4}$$

and for the $L1_2$-type alloys the APB energy $E_{\rm APB}$ is written by using the quasichemical approximation of Yang,[10]

$$E_{\rm APB}=\frac{1.41k_BT_c}{a^2} \ , \tag{5}$$

where G is the shear modulus, ψ is the angle between the normal direction of the dislocation line and its Burgers vector, ν is Poisson's ratio, k_B is the Boltzmann constant, and T_c is the critical temperature of the atomic order-disorder transition.

For the b-type superlattice dislocations, the number of B atoms at the irregular site is written as

$$n=\frac{S^2}{\sqrt{3}a^2}\sqrt{\rho} \ . \tag{6}$$

Next, the effect of partial dislocations is considered. As shown in Fig. 2, one perfect dislocation separates into two partial dislocations over the (111) glide plane. We have

$$\frac{a}{2}[01\bar{1}]=\frac{a}{6}[11\bar{2}]+\frac{a}{6}[\bar{1}2\bar{1}] \ . \tag{7}$$

The stacking fault and APB extend between the partial dislocations as shown in Fig. 2. In the regions (a) and (c), B-B atom pairs align along $(a/6)[114]$ and $(a/6)[141]$, respectively. The number of B atoms on the irregular sites is given as

$$n=\frac{S^2}{\sqrt{3}a^2}\bar{r}_1\rho' \ , \tag{8}$$

where $\bar{r}_1$ is the average of r_1 and ρ' is the density of partial dislocations whose ρ value is twice that of the perfect dislocation's ρ. $\bar{r}_1$ is expected to be much smaller than $\bar{r}$. The effect of partial dislocations would be neglected henceforth.

III. MAGNETIC TRANSITION CAUSED BY PLASTIC DEFORMATION

There are many alloys with the $L1_2$-type structure which show the different magnetic behaviors in the chemically ordered and disordered states. The neighboring environments of each atom are different in these states. The magnetic interactions between atoms are intimately related with the atomic environment. The Pt_3Fe alloy, for instance, is antiferromagnetic in the fully ordered state, while the coexistence of ferromagnetic and antiferromagnetic states is observed in the disordered state.[1,2] As another example, the Ni_3Mn alloy has the ferromagnetic structure in the ordered state and the antiferromagnetic structure in the disordered state.[11,12]

Plastic deformation produces the different atomic environment. A and B atoms exchange their sites with each other along the APB. Figure 3 shows the atomic arrangement of the $L1_2$-type structure, in which the $(a/2)[\bar{1}10]$ dislocation slips over the (111) glide plane and places the APB there. A atoms exchange their sites with B atoms in both sides of the APB and B atoms on one side of the APB (at the corner sites in Fig. 3) become irregular for A atoms in the other side. On the (111) APB there are two kinds of A atoms with different atomic environment. The first kind of A atoms occupy the F sites (at the face-centered sites in Fig. 3), where they have the same number of the A and B atoms as those of the normal state in their each NN, although the arrangement of the atoms around the host A atoms changes in the first, third, and fifth NN (Table I). The second kind of A atoms occupy the C sites (the corner site in Fig. 3) and have more neighboring A atoms than those of the normal state in the first, third, and fifth NN, but the B atoms appear in the second, fourth, and sixth NN of the host A atoms at the C sites (Table I). The probability that the A atoms occupy the C sites is $\frac{1}{3}$.

The atomic environment changes by plastic deformation and then the magnetic couplings change. For example, by applying cold work to the Pt_3Fe alloy which showed no ferromagnetism, a strong ferromagnetism was observed even at room temperature.[1] It was also found that plastic deformation causes the Ni_3Mn alloy to reduce the magnetization and that in the ordered Pt_3Co alloy, the intensity of magnetization increases with the amount of compression.[3] The other example of the magnetic transition on plastic deformation was observed in the Ni_3Al compound.[4] These phenomena were understood from the viewpoint of the new disordered regions produced during plastic deformation.

Before plastic deformation, the magnetization of the fully ordered A_3B alloy and/or compound at 0 K is written as

$$\vec{M}(0)=3N_0\vec{\mu}_\alpha+N_0\vec{\mu}_\beta \ , \tag{9}$$

where N_0 is the total number of B atoms and $\vec{\mu}_\alpha$ and $\vec{\mu}_\beta$ are magnetic moments of A and B atoms occupying their own regular sites, respectively. The application of cold work forms an APB over the glide plane, across which the atoms exchange their own sites with each other (Table I). With plastic deformation advancing, the number of atoms

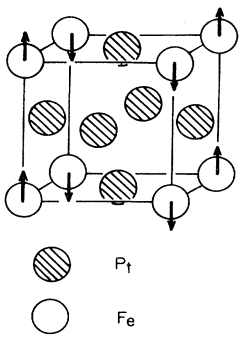

FIG. 4. Atomic arrangement and magnetic structures for the ideal stoichiometric Pt_3Fe alloy. Open circles represent iron atoms and shaded circles represent platinum atoms.

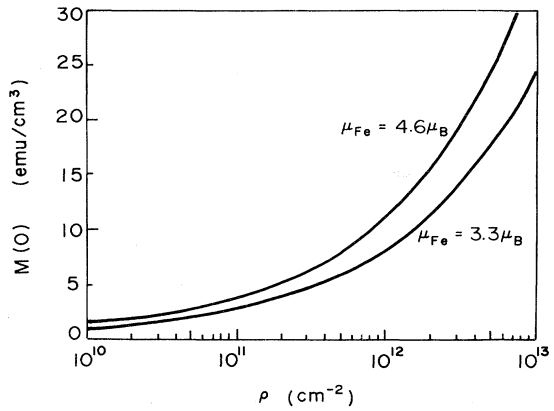

FIG. 5. Relationship between the magnetization at 0 K, $M(0)$, and the dislocation density ρ, in the plastically deformed Pt_3Fe alloy. Relationship is estimated for the advanced stage of plastic deformation where the b-type superlattice dislocations are the main distributors.

at the irregular sites is augmented according to Eqs. (3) and (6). The net magnetization of the plastically deformed A_3B alloy and/or compound at 0 K is given by

$$\vec{M}(0)=3(N_0-N)\vec{\mu}_\alpha+(N_0-N)\vec{\mu}_\beta +2N\vec{\mu}_\alpha^F+N\vec{\mu}_\alpha^C+N\vec{\mu}_\beta', \quad (10)$$

where N is the number of B atoms near the APB which have a different environment from the normal state and have the magnetic moment $\vec{\mu}_\beta'$. $\vec{\mu}_\alpha^i$ is the magnetic moment of A atoms with the different environment near the APB. The superscripts F and C mean the irregular F and C sites, respectively. N will increase in proportion to the dislocation density at the early stage of plastic deformation and to the square root of it at the advanced stage. The magnetization will change with plastic deformation.

A. Pt_3Fe alloy

In the perfect structure of the ideal stoichiometric Pt_3Fe alloy the magnetic interaction between second-NN Fe-Fe atom pairs is antiferromagnetic and Pt atoms have no magnetic moment in this alloy.[1] The magnetic structure is illustrated in Fig. 4. It consists of the ferromagnetic (110) sheets of atoms which are arranged antiferromagnetically. As all the spins of Fe atoms are coupled with themselves, half the Fe spins would be situated one way and the other half would have a zero net magnetization in the completely ordered state and thus they make no contribution to the magnetization.

In the plastically deformed alloy, Fe-Fe atom pairs appear in the first NN across the APB over the glide plane. These Fe-Fe atom pairs bring about strong ferromagnetism. The number of Fe atoms which are ferromagnetically coupled near the APB is given by $N=2n/3$. The numerical coefficient $\frac{2}{3}$ derives from the fact that each Fe atom is surrounded by the six second-NN Fe atoms and two-thirds of them are antiferromagnetically coupled and one-third is ferromagnetically coupled (Fig. 4). Two-thirds of the Fe atoms change their coupling on plastic deformation from antiferromagnetic to ferromagnetic along the APB.

We assume that the magnitude of magnetic moment of Fe and Pt atoms at their irregular sites is the same as that at their regular sites and $\mu'_{Fe}=3.3\mu_B$ and $\mu_{Pt}^F=\mu_{Pt}^C=0.0\mu_B^2$. The magnetization of the plastically deformed Pt_3Fe alloy is shown as a function of the dislocation density over the range 10^{10}–10^{13} cm^{-2}. Here $a=3.864$ Å is adopted.[13] This relationship is illustrated for the b-type superlattice dislocations because this range of ρ corresponds to the advanced stage of plastic deformation (Fig. 5).

In the Crangle's study[1] the specimens were crushed into powder by means of a file, and the strong magnetization was observed. X-ray examination also showed that the superlattice reflections were not observed in the powdered specimens, and the annealing not only restored the superlattice reflections but also removed the ferromagnetism. These experiments would be consistent with our phenomenological model. His study suggested that if the magnetization were attributed entirely to Fe atoms, the Fe atoms would each have a moment of $4.6\mu_B$. The APB extends 10^{-4} cm and 10^{-6} cm in width and length, respectively, over the glide plane, making a "stripe." The thousands of Fe atoms are arrayed across an APB stripe, as they are ferromagnetically coupled. These Fe atoms would be considered to make a magnetic cluster and have a very large magnetic moment. Then the relationship between the magnetization and the dislocation density is included in Fig. 5, assuming $\mu_{Fe}=4.6\mu_B$.

B. Ni_3Mn alloy

In the Ni_3Mn alloy, the Mn-Mn coupling has been probed by many investigators.[11,12,14] Mn atoms coupled ferromagnetically at the second-NN distance in the ordered state. The coexistence of the ferromagnetic and antiferromagnetic couplings was observed in the disordered state. There is a weak positive exchange interaction between the first-NN Ni-Ni atom pairs while the interaction between the first-NN Ni-Mn pairs is relatively strong and also positive. On the other hand, the exchange interaction between the first-NN Mn-Mn atom pairs is very strongly negative.[14,15] Thus, for a perfectly ordered Ni_3Mn alloy

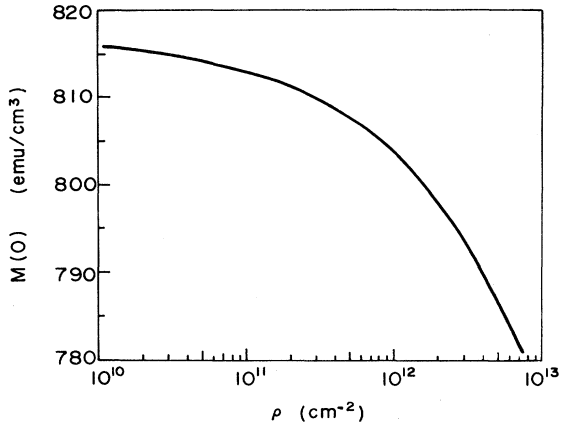

FIG. 6. Relationship of the magnetization at 0 K, $M(0)$, and the dislocation density ρ, in the plastically deformed Ni_3Mn alloy. b-type superlattice dislocations are the main distributors.

there will be no first-NN Mn-Mn pairs and no Mn atoms in the antiparallel direction. Plastic deformation changes the atomic arrangement at their own sites. Across the APB over the glide plane, Mn-Mn atom pairs appear at the first NN (Table I).

It was found that the saturation magnetization decreases with increasing plastic deformation. The decrease of magnetization was understood with consideration that the new disordered regions are produced during plastic deformation.[3] The net magnetization is estimated versus the dislocation density, supposing $S=1$, and $\mu'_{Mn}=-\mu_{Mn}=-3.18\mu_B$ and $\mu^F_{Ni}=\mu^C_{Ni}=0.3\mu_B$.[16,17] In Fig. 6 the magnetization is shown versus the dislocation density over the range 10^{10}–10^{13} cm^{-2}, where $a=3.59$ Å (Ref. 18) and the b-type superlattice dislocations are main distributors.

C. Pt_3Co and Ni_3Fe alloys

The Pt_3Co and Ni_3Fe alloys are ferromagnetic in both the ordered and disordered states. Both have different Curie temperatures in the ordered and disordered states. The magnetic moments on the Pt and Co atoms or the Ni and Fe atoms are different in these states.[19,20] The result suggested that the interatomic exchange interactions are important in these alloys.

It was found[3] in the ordered Pt_3Co alloy that the disordering due to plastic deformation enhances the magnetization, and the increase in magnetization was roughly proportional to the amount of plastic deformation. Through plastic deformation the area of the APB increases over the glide plane and the number of Pt and Co atoms at the irregular sites increases according to Eqs. (3) and (6). If the magnetic moments of these atoms at the irregular sites were the same as those in the disordered state determined by Menzinger and Paoletti,[19] the enhancement of magnetization upon plastic deformation would be more easily elucidated. The net magnetization at 0 K against the dislocation density will be estimated under a few assumptions. Equation (10) will be rewritten as

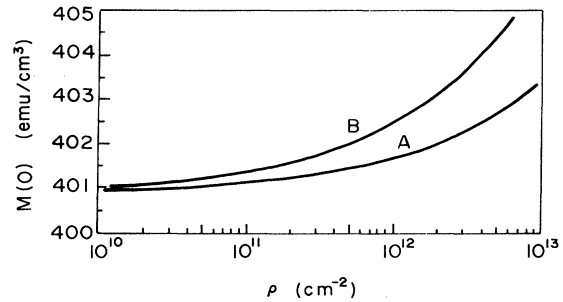

FIG. 7. Relationship between the magnetization at 0 K, $M(0)$, and the dislocation density ρ, in the plastically deformed Pt_3Co alloy. b-type superlattice dislocations are the main distributors. Curves A and B correspond to assumptions (A) and (B), respectively.

$$M(0)=N_0\mu_0+N(\mu'_0-\mu_0)\ , \tag{11}$$

where μ_0 and μ'_0 are the values of the magnetic moment per unit cell in the fully chemically ordered and disordered states, respectively. Assuming that the influence of the environment of the atoms due to plastic deformation is considered as far as in the second NN, then $N=n$ [assumption (A)]. On the other hand, if the influence extends as far as to the fourth NN, $N=2n$ [assumption (B)]. Figure 7 shows the magnetization at 0 K of the Pt_3Co alloy deformed plastically for the two assumptions. The b-type superlattice dislocations are main distributors. Here $S=1$, $\mu_0=(2.43\pm0.03)\mu_B$, $\mu'_0=(2.65\pm0.03)\mu_B$,[19] and $a=3.831$ Å (Ref. 21) are adopted. If the environment of atoms farther inside than the sixth NN influences the magnetic behavior, the magnetization would increase more rapidly than in Fig. 7.

The relation between the magnetization and the dislocation density in the Ni_3Fe alloy can be obtained by the same method as in Pt_3Co alloy. The magnetizations in the ordered and disordered states are 972 and 927 G, respectively.[20] The Ni and Fe atoms at the irregular sites along the APB would have the same magnetic moment as those in the disordered state. If the influence of environment of the atoms due to plastic deformation extends as far as the second NN, the relationship between the magnetization and dislocation density is estimated in the

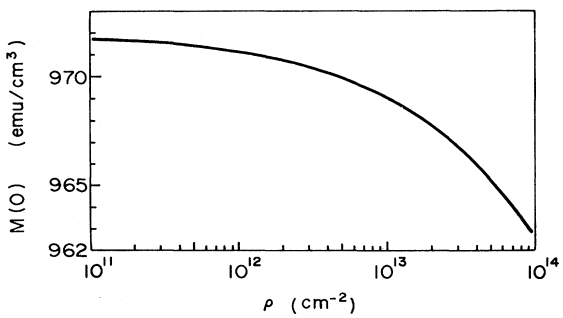

FIG. 8. Relationship of the magnetization at 0 K, $M(0)$, and the dislocation density ρ, in the plastically deformed Ni_3Fe alloy. b-type superlattice dislocations are the main distributors.

Ni_3Fe alloy. The relation is shown in Fig. 8, where $a = 3.5544$ Å,[22] b-type superlattice dislocations are main distributors, and $S = 1$ is supposed.

The influence of plastic deformation does not appear remarkable regarding the magnetization but appears so on the magnetic anisotropy predominantly in the Ni_3Fe alloy. The magnetic anisotropy induced by plastic deformation is well known as "roll-induced magnetic anisotropy."[23] The mechanism of the anisotropy was explained well by Chikazumi *et al.*[24] initially from the viewpoint of the atom-pair model.[25,26,27] The "slip-induced directional-order model" was modified and the magnitude of the roll-induced magnetic anisotropy increases in proportion to n in Eqs. (3) and (6).[6] This result has been experimentally confirmed.[7,28]

D. Ni_3Al compound

It was concluded in the paper by De Boer *et al.*[4] that the Ni_3Al intermetallic compound shows very weak itinerant ferromagnetism as an example of the Stoner-Edwards-Wohlfarth model. They showed that the disordering due to plastic deformation causes the susceptibility, as well as the magnetization, to decrease considerably, and also demonstrated that plastic deformation brings about a decrease of the intensity of the superlattice x-ray reflection. The disordered state is concluded to be paramagnetic. These results were in accordance with the Mössbauer-effect measurements, and the paramagnetic state remains intact until 4 K is reached.[29]

The magnetic properties of this compound are highly sensitive to the concentration. That is, $Ni_{74}Al_{26}$ is paramagnetic but $Ni_{75}Al_{25}$ is ferromagnetic. The excess Al atoms occupy the Ni sites in the Al-rich $Ni_{3-x}Al_{1+x}$ compound, and it will be possible to consider that the substitutional Al atoms at the Ni sites cause the neighboring Ni atoms to be paramagnetic. The critical concentration of the transition from ferromagnetism to paramagnetism becomes $x = 3/(p+1)$, where p is the number of neighboring Ni atoms which change their magnetic moments to be paramagnetic by one substitutional Al atom. One can find that the excess Al atoms influence their neighboring Ni atoms as far as at least to the sixth NN in the magnetic transition.

By plastic deformation the Ni atoms exchange their sites with Al atoms in both sides of the APB and the Al atoms in one side of the APB (at the corner sites in Fig. 3) become irregular for the Ni atoms in the other side (at C sites). These Al atoms will cause the magnetic moment of the neighboring Ni at the C sites to become paramagnetic with the same reason as the substitutional Al atoms in the $Ni_{3-x}Al_{1+x}$ compound with $x > 0$. The Ni atoms at F sites have a different environment from those in the normal state and they also possibly behave paramagnetically as well as at the C site.

As shown in Table I, the Ni atoms at F sites have the same number of the neighboring Ni and Al atoms as in the normal state on each NN, whereas for the Ni atoms, at C sites the Al atoms appear on their second, fourth, and sixth NN. Considering the disappearance of ferromagnetism in the Al-rich Ni_3Al compound, the Ni atoms at C sites near the APB must behave paramagnetically. If the influence of the change of environment around the Ni atoms extends as far as to the sixth NN, then $N = 3n$, $\mu_{Ni}^{C} = 0$, and $\mu_{Ni}^{F} = \mu_{Ni}$ will be satisfied [assumption (C)].

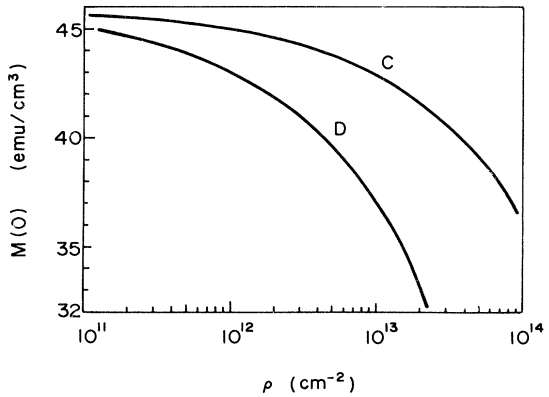

FIG. 9. Relationship of the magnetization at 0 K, $M(0)$, and the dislocation density ρ, in the plastically deformed Ni_3Al compound. Curves C and D correspond to assumptions (C) and (D), respectively.

Though the Ni atoms at F sites have the same number of neighboring Ni and Al atoms as those in the normal state on each NN, the arrangement of the neighboring atoms around these Ni atoms is different from that in the normal state. Thus, the Ni atoms at F sites possibly behave paramagnetically as well as at C sites because of the change of electronic structure due to the destruction of the symmetry of atomic environment. When not only the number of Al atoms on each NN but also their arrangement, is concerned with the origin of the weak ferromagnetism of this compound, all the Ni atoms on and near the APB will behave paramagnetically. If the influence extends as far as to the sixth NN, then $N = 3n$, $\mu_{Ni}^{F} = 0$, and $\mu_{Ni}^{C} = 0$ [assumption (D)].

Figure 9 shows the magnetization at 0 K in the plastically deformed Ni_3Al compound, which is calculated under two assumptions. The b-type superlattice dislocations are main distributors. Here $\mu_{Ni} = 0.075\mu_B$ (Ref. 4) and $a = 3.570$ Å (Ref. 30) are adopted. If the environment of Ni atoms farther inside than the sixth NN influences the magnetic behaviors, then the magnetization would decrease more rapidly than in Fig. 9.

The influence of plastic deformation on magnetic properties has not been studied in the ordered alloys with a few exceptions. And the effects of plastic deformation have been avoided by annealing as the complicated phenomena. But it may be possible to study the magnetic localized phenomena in light of the new aspects by use of the present results. The present results might be applied to the other alloys with the other structure as well as the $L1_2$-type structure. An experimental study on the present theme is at present in progress.

*Permanent address: Faculty of Engineering, Iwate University, Morioka, Iwate, Japan.

[1]J. Crangle, J. Phys. Radium 20, 435 (1959).
[2]G. E. Bacon and J. Crangle, Proc. R. Soc. London Ser. A 272, 387 (1963).
[3]T. Taoka, K. Yasukōchi, R. Honda, and I. Ōyama, J. Phys. Soc. Jpn. 14, 888 (1959).
[4]F. R. De Boer, C. J. Shinkel, J. Biesterbos, and S. Proost, J. Appl. Phys. 40, 1049 (1969).
[5]T. Shinohara, K. Sasaki, H. Yamauchi, H. Watanabe, H. Sekizawa, and T. Okada, J. Phys. Soc. Jpn. 50, 2904 (1981).
[6]S. Takahashi, Phys. Status Solidi A 42, 201 (1977).
[7]S. Takahashi, Phys. Status Solidi A 42, 529 (1977).
[8]S. Takahashi and T. Shinohara, J. Phys. F 12, 3115 (1982).
[9]M. J. Marcinkowski and N. Brown, Acta Metallurg. 9, 764 (1961).
[10]C. N. Yang, J. Chem. Phys. 13, 66 (1945).
[11]M. J. Marcinkowski and N. Brown, J. Appl. Phys. 32, 375 (1961).
[12]V. R. Hahn and E. Kneller, Z. Metallkunde. 49, 426 (1958).
[13]G. E. Bacon and S. A. Willson, Proc. Phys. Soc. London 82, 620 (1963).
[14]W. J. Carr, Jr., Phys. Rev. 85, 590 (1952).
[15]H. Sato, in *Proceedings of the International Conference on Magnetism and Magnetic Materials* (AIEE, New York, 1955), p. 119.
[16]J. S. Kouvel, C. D. Graham, Jr., and I. S. Jacobs, J. Phys. Radium 20, 198 (1959).
[17]W. Proctor, R. G. Scurlock, and E. M. Wray, Proc. Phys. Soc. London 90, 697 (1967).
[18]B. L. Averbach, J. Appl. Phys. 22, 1088 (1951).
[19]F. Menzinger and A. Paoletti, Phys. Rev. 143, 365 (1966).
[20]T. Taoka and T. Ohtsuka, J. Phys. Soc. Jpn. 9, 712 (1954).
[21]A. H. Geisler and D. L. Martin, J. Appl. Phys. 23, 375 (1952).
[22]R. J. Wakelin and E. L. Yates, Proc. Phys. Soc. London Sec. B 66, 221 (1953).
[23]W. Six, J. L. Snoek, and W. Burgers, De Ingenier 49, E195 (1934).
[24]S. Chikazumi, K. Suzuki, and H. Iwata, J. Phys. Soc. Jpn. 12, 1295 (1957).
[25]L. Néel, J. Phys. Radium 15, 225 (1945).
[26]L. Néel, C. R. Acad. Sci. (Paris) 238, 305 (1954).
[27]S. Taniguchi and M. Yamamoto, Sci. Rep. Res. Inst. Tôhoku Univ. A 6, 330 (1954).
[28]S. Takahashi, Phys. Status Solidi A 45, 133 (1978).
[29]J. K van Deen, J. W. Drijver, and F. van der Woude, Physica 86-88B, 397 (1977).
[30]R. W. Guard and J. H. Westbrook, Trans. AIME 215, 871 (1959).